Published in final edited form as:

Virology. 2012 April 25; 426(1): 22–33. doi:10.1016/j.virol.2011.11.022.

Mutational analysis of the West Nile virus NS4B protein

Jason A. Wicker[a,b,1,2], **Melissa C. Whiteman**[b,2], **David W.C. Beasley**[a,b], **C. Todd Davis**[b,3], **Charles E. McGee**[b], **J. Ching Lee**[c], **Stephen Higgs**[d], **Richard M. Kinney**[e], **Claire Y.-H. Huang**[e], and **Alan D.T. Barrett**[a,b,*]

[a] Department of Microbiology and Immunology, Sealy Center for Vaccine Development, Center for Biodefense and Emerging Infectious Diseases, Sealy Center for Structural Biology and Molecular Biophysics, and Institute for Human Infections and Immunity, University of Texas Medical Branch at Galveston, TX 77555-0609, USA

[b] Department of Pathology, Sealy Center for Vaccine Development, Center for Biodefense and Emerging Infectious Diseases, Sealy Center for Structural Biology and Molecular Biophysics, and Institute for Human Infections and Immunity, University of Texas Medical Branch at Galveston, TX 77555-0609, USA

[c] Department of Biochemistry and Molecular Biology, Sealy Center for Vaccine Development, Center for Biodefense and Emerging Infectious Diseases, Sealy Center for Structural Biology and Molecular Biophysics, and Institute for Human Infections and Immunity, University of Texas Medical Branch at Galveston, TX 77555-0609, USA

[d] Biosecurity Research Institute, Kansas State University, Manhattan, KS 66506-2902, USA

[e] Division of Vector-Borne Viral Diseases, Centers for Disease Control and Prevention, Public Health Service, U.S. Department of Health and Human Services, Fort Collins, CO 80521, USA

Abstract

West Nile virus NS4B is a small hydrophobic nonstructural protein approximately 27 kDa in size whose function is poorly understood. Amino acid substitutions were introduced into the NS4B protein primarily targeting two distinct regions; the N-terminal domain (residues 35 through 60) and the central hydrophobic domain (residues 95 through 120). Only the NS4B P38G substitution was associated with both temperature-sensitive and small-plaque phenotypes. Importantly, this mutation was found to attenuate neuroinvasiveness greater than 10,000,000-fold and lower viremia titers compared to the wild-type NY99 virus in a mouse model. Full genome sequencing of the NS4B P38G mutant virus revealed two unexpected mutations at NS4B T116I and NS3 N480H (P38G/T116I/N480H), however, neither mutation alone was temperature sensitive or attenuated in mice. Following incubation of P38G/T116I/N480H at 41 °C, five mutants encoding compensatory substitutions in the NS4B protein exhibited a reduction in the temperature-sensitive phenotype and reversion to a virulent phenotype in the mouse model.

* Corresponding author at: Department of Pathology, University of Texas Medical Branch, Galveston, TX 77555-0609, USA. Fax: +1 409 772 6663. abarrett@utmb.edu (A.D.T. Barrett)..

[1]Present address: Department of Pathology, University of Alabama-Birmingham, Birmingham, AL 35233, USA.

[2]JAW and MCW contributed equally to the paper.

[3]Present address: Influenza Division, Molecular Virology and Vaccines Branch, NCIRD, Centers for Disease Control & Prevention, Atlanta, GA 30333, USA.

Keywords

West Nile virus; *Flavivirus*; NS4B protein; Attenuated phenotype; Temperature sensitivity

Introduction

West Nile virus (WNV) is a mosquito-transmitted member of the genus *Flavivirus*, family *Flaviviridae*. This genus includes other mosquito-borne viruses of public health importance: yellow fever virus (YFV), Japanese encephalitis virus (JEV), and the four dengue viruses (DENV-1–DENV-4). The WNV genome is a single-stranded, positive-sense RNA molecule approximately 11 kb in length encoding a single polyprotein that is co- and post-translationally cleaved by a combination of viral and host proteases to produce three structural (C, prM, and E) and seven nonstructural (NS) proteins (NS1, NS2A, NS2B, NS3, NS4A, NS4B, and NS5) (Brinton, 2002; Mukhopadhyay et al., 2005). While two of the nonstructural proteins, the NS5 polymerase and NS3 protease, have been relatively well-characterized, the structure and function of the remaining nonstructural proteins, NS1, NS2A, NS2B, NS4A, and NS4B, remain poorly defined (Khromykh et al., 1999; Mastrangelo et al., 2007). Within the family *Flaviviridae*, WNV NS4B exhibits approximately 35% amino acid identity with other mosquito-borne flaviviruses (Umareddy et al., 2006), such as YFV and members of the DENV serogroup (Fig. 1A). Amino acid identities are higher with more closely related viruses such as St. Louis encephalitis virus (SLEV) and JEV with values of 56% and 65%, respectively. The most genetically divergent WNV isolate, known as Rabensburg virus, displays 88% amino acid identity with NY99 WNV in NS4B (Bakonyi et al., 2005). Accumulation of NS4B in the perinuclear region along with induction of membrane proliferation has been described in WNV (subtype Kunjin)-infected cells, and there is evidence that NS4B can translocate into the nucleus (Westaway et al., 1997). Flaviviral NS4B was also found to inhibit the interferon-signaling cascade at the level of nuclear STAT phosphorylation and has been implicated in modulation of the stress-induced unfolded protein response (Ambrose and Mackenzie, 2011; Munoz-Jordan et al., 2003, 2005). Amino acid residues in the N-terminal region of the WNV NS4B protein have been shown to control interferon resistance in HeLa cells expressing subgenomic replicons, although no effect was shown on the expression of full-length infectious genomes (Evans and Seeger, 2007). NS4B has also been found to co-localize with other components of the viral replication complex, such as NS3 and double-stranded RNA (Miller et al., 2006). Sequential processing of the 2 K signal fragment between the NS4A and NS4B proteins is thought to be critical for the induction of cytoplasmic membrane alterations allowing for replication complex formation and maturation of individual proteins (Miller et al., 2007; Preugschat and Strauss, 1991; Roosendaal et al., 2006). Secondary structure predictions of the flavivirus NS4B protein generated by the consensus ConPredII hydrophobicity plotting program suggest that it is a very hydrophobic protein with five transmembrane domains (Arai et al., 2004) (Fig. 1B). Experimental evidence suggests that there are three membrane-spanning domains in the DENV-2 NS4B protein that are capable of targeting a cytosolic marker protein to intracellular membranes while the two N-terminal putative trans-membrane domains

predicted by some computer programs may not be biologically significant (Miller et al., 2006).

Previous studies have described mutations in the NS4B protein of attenuated or passage-adapted mosquito-borne flaviviruses, including WNV (Davis et al., 2004; Puig-Basagoiti et al., 2007), suggesting that this protein plays an important role in replication and pathogenesis. In the case of other flaviviruses, a single coding mutation (P101L) in DENV-4 NS4B conferred a small-plaque phenotype in *Aedes albopictus* (C6/36) cells, while at the same time increasing plaque size in mammalian Vero and Huh-7 cells two-fold and three-fold, respectively, when assayed via immunoperoxidase staining (Hanley et al., 2003). Subsequent studies have suggested that DENV-4 NS4B interacts with the NS3 protease and that the P101L substitution ablates this interaction (Umareddy et al., 2006). Pletnev et al. described DENV-4 NS4B T105I and L112S substitutions that occurred in a chimeric virus expressing WNV structural proteins in a DENV-4 backbone (Pletnev et al., 2002). Blaney et al. identified a NS4B L112F mutation in a DENV-4 passaged in Vero cells, while the live attenuated JEV vaccine strain SA14-14-2 has an I106V substitution in NS4B (Blaney et al., 2003; Ni et al., 1995). A hamster viscerotropic Asibi strain of YFV, generated by seven passages through hamsters, accumulated seven amino acid substitutions in the polyprotein, including a V98I substitution in NS4B (McArthur et al., 2003). Interestingly, YFV vaccine strains also display a mutation in NS4B at I95M (Hahn et al., 1987; Wang et al., 1995). When the NS4B proteins from different flaviviruses are aligned, it becomes clear that these mutations are all located in a similar central hydrophobic region of the protein (Fig. 1A).

In this study, amino acid substitutions were engineered into either the central hydrophobic region of the WNV NY-99 strain NS4B protein or an N-terminal motif that is highly conserved in both tick-borne and mosquito-borne flaviviruses. In total, eight amino acid substitutions were engineered into distinct regions of the WNV NS4B protein. While most mutations had no detectable effect on the phenotypic properties examined, the mutant containing a P38G substitution was found to confer a small-plaque phenotype in cell culture and attenuation of the neuroinvasive phenotype in mice.

Results

Design of amino acid substitutions

The alignment in Fig. 1A shows a series of highly conserved amino acids in the N-terminal portion of NS4B from both mosquito- and tick-borne flaviviruses. For WNV these residues corresponded to D35, P38, W42, and Y45. The W42 and Y45 residues are perfectly conserved in all mosquito- and tick-borne flaviviruses based on available sequence data. The D35 residue is found in every mosquito- or tick-borne flavivirus examined except for the Brazilian mosquito-borne flaviviruses Ilheus and Rocio, which encoded an alanine and glutamic acid residue, respectively (Kuno and Chang, 2005). The P38 residue is conserved in every flavivirus examined except for Ilheus virus, which encoded an alanine at this residue. Utilizing the ConPredII consensus topology modeling program, the WNV P38 residue is predicted to reside near the junction of an endoplasmic reticulum lumenal and transmembrane domain (Arai et al., 2004). To determine the importance of these residues in viral multiplication and virulence phenotypes, D35E, P38G, W42F, and Y45F mutations

were engineered into the WNV NS4B protein via site-directed mutagenesis of an infectious clone. Amino acid substitutions were selected on the basis of a combination of either conservative substitutions or substitutions identified in one or more strains of different flaviviruses at the specific residue.

Previous studies have described amino acid substitutions in a central hydrophobic region of NS4B in either attenuated or passage-adapted flavivirus strains (Hanley et al., 2003; McArthur et al., 2003; Wicker et al., 2006). Examination of alignments of various flaviviral NS4B amino acid sequences (Fig. 1A), revealed that these mutations all localized to a distinct region, residues 95–120. While amino acid identities of flaviviruses were variable in this region, there was a high concentration of hydrophobic residues, suggesting that some of these residues may interact with intracellular membranes. Amino acid substitutions in WNV NS4B were engineered at homologous positions corresponding to published flaviviral NS4B mutations. WNV L97M and A100V substitutions corresponded to mutations identified in attenuated (M95I) or passage adapted (V98I) YFV strains (Hahn et al., 1987; McArthur et al., 2003; Wang et al., 1995). In addition, the engineered WNV NS4B L108P substitution was homologous to the DENV-4 P101L mutation found to confer a selective advantage in mammalian Vero and Huh7 cells (Hanley et al., 2003). Thus, recombinant WN viruses were produced containing individual L97M, A100V, and L108P mutations to determine if mutations associated with attenuation of other flaviviruses conferred attenuation of either cellular multiplication or mouse virulence phenotypes in WNV. A T116I substitution was also introduced following the identification of this additional mutation in a recombinant virus encoding a designed P38G substitution to determine its role in observed viral phenotypes.

Rescue of recombinant viruses

Utilizing site-directed mutagenesis and the two-plasmid infectious clone of WNV NY99 (Beasley et al., 2005; Kinney et al., 2006), mutant viruses containing either D35E, P38G, W42F, Y45F, L97M, A100V, L108P, or T116I substitutions in the NS4B protein were rescued following transfection of Vero cells. Sequencing of the NS4B region of recombinant viruses was conducted to confirm the presence of the mutation of interest. No other nucleotide changes were identified in any virus, except for P38G virus. Virus stocks produced from the initial transfection were used for all subsequent studies with the exception of this P38G virus. Following multiple transfection experiments, titers of P38G virus were not sufficiently high (approximately 2 $\log_{10}$ pfu/mL) for subsequent studies, so this virus was passaged once in Vero cells. Upon sequencing of the NS4B region, the P38G virus was found to contain additional NS4B T116I and NS3 N480H substitutions that were not present in the original DNA plasmid, so this virus will henceforth be denoted as P38G/T116I/N480H. A single T116I or N480H substitution was engineered into the WNV infectious clone to test the relative contribution towards observed phenotypes of this mutation outside the context of the P38G mutation. The T116I mutant displayed a plaque phenotype similar to wild type virus. The P38G/T116I/N480H mutant virus was found to exhibit a small-plaque phenotype when compared to wild-type or other mutant viruses (less than 1 mm versus 4 mm for the parental virus) (data not shown). The N480H mutant

displayed an intermediate plaque phenotype compared to the NY99 wild type and P38G/T116I/N480H viruses.

Temperature sensitivity and multiplication kinetics of recombinant viruses in cell culture

Each recombinant mutant virus was investigated for temperature sensitivity by plaquing in Vero cells at both 37 °C and 41 °C. D35E, W42F, Y45F, L97M, A100V, L108P, T116I, and N480H mutant viruses and wild-type all showed similar levels of plaquing efficiency at both temperatures (Table 1). In contrast, the P38G/T116I/N480H virus was found to exhibit a 3.8 $\log_{10}$ pfu reduction in efficiency of plaquing at 41 °C compared to 37 °C (Table 1A) while there was no reduction in plaquing efficiency in Vero cells at 39.5 °C (data not shown).

Multiplication curves of wild-type WNV NY-99 and the mutant viruses were compared at a moi of 0.01 in Vero cells at both 37 °C and 41 °C (Fig. 2). In addition, multiplication curves of recombinant viruses in mouse neuroblastoma Neuro2A at 37 °C and mosquito C6/36 cells at 28 °C were undertaken (data not shown). All mutant viruses were indistinguishable from wild-type virus in each cell line tested with the exception of the P38G/T116I/N480H virus. The P38G/T116I/N480H virus exhibited a significant delay in multiplication in Vero cells at 41 °C, but not at 37 °C (Figs. 2A and 2C). Infectivity titers for the P38G/T116I/N480H virus at 41 °C were also significantly lower than those for wild-type virus at every time point except 96 h. The P38G/T116I/N480H virus showed no differences in multiplication kinetics from wild-type virus in Neuro2A and C6/36 cells at the temperatures tested (data not shown).

P38G/T116I/N480H virus is attenuated for neuroinvasiveness but not neurovirulence in mice

We have previously described a mouse model to investigate neuroinvasiveness and neurovirulence of WNV via inoculation of 3–4 week-old female NIH Swiss mice intraperitoneally (ip) or intracerebrally (ic), respectively (Beasley et al., 2002). With the exception of the P38G/T116I/N480H virus, all recombinant viruses were as virulent as wild-type WNV following ip inoculation in terms of lethality and average survival time (Table 1). The P38G/T116I/N480H mutant was attenuated for neuroinvasiveness with an ip LD_{50} value of greater than 10,000 pfu. However, when inoculated via the ic route, the P38G/T116I/N480H mutant remained as lethal as wild-type WNV with an ic LD_{50} value of less than 0.1 pfu.

The P38A substitution maintained a neuroinvasive phenotype in mice

Following identification of the attenuated P38G/T116I/N480H virus, a P38A amino acid substitution was introduced into the WNV infectious clone to better elucidate the importance of the P38 residue in the absence of other amino acid mutations. The P38 residue is conserved in both mosquito- and tick-borne flaviviruses except for Ilheus virus, which encoded an alanine at this residue (Fig. 1A). Recombinant mutant WNV encoding the P38A substitution was not temperature sensitive and exhibited a mouse neuroinvasive phenotype comparable to wild-type WNV (Table 1A).

Multiplication of P38G/T116I/N480H virus in mice

Multiplication kinetics were compared in mice following ip inoculation of either 100 pfu wild-type WNV or 100 pfu P38G/T116I/N480H mutant in the NIH Swiss mouse model to determine serum and brain infectivity titers for these viruses. The peak viremia for wild-type WNV occurred on day 2 post-inoculation and reached 5.0 $\log_{10}$ pfu/mL, while the peak titer for the P38G/T116I/N480H virus was 3.1 $\log_{10}$ pfu/mL, also on day 2 post-inoculation (Table 2). Peak brain titers reached 6.8 $\log_{10}$ pfu for the wild-type virus on day 6 post-inoculation while virus infection was never detected in the brains of P38G/T116I/N480H infected mice. The limit of detection was 1.7 $\log_{10}$ pfu/mL for serum and 2.7 $\log_{10}$ pfu/brain for the brain. RT-PCR amplification was conducted on RNA isolated from mouse brain on day 6, when high titers of wild-type WNV were detected in the brain. No PCR product was detected for WNV RNA from brains of mice infected with P38G/T116I/N480H virus, while the brains of mice infected with wild-type virus were positive for viral RNA (data not shown). Thus, while the P38G/T116I/N480H virus exhibited detectable serum infectivity titers, there was no evidence the virus ever invaded the brain.

Isolation of P38G/T116I/N480H derivatives encoding compensatory mutations

As shown in Fig. 2C, the P38G/T116I/N480H virus exhibited delayed multiplication in Vero cells at 41 °C with infectivity titers finally approaching those of wild-type virus by 96 h post-infection. Given that a pattern characteristic of delayed multiplication was observed, a virus sample from the 96-hour time point was investigated to test for the selection of virus that was either a revertant or contained compensatory mutations. Serial dilutions of P38G/T116I/N480H-derived virus grown in Vero cells at 41 °C from the 96-hour time point were inoculated via the ip route into female three-week-old NIH Swiss mice to test for virulence characteristics of the virus. Sporadic mortality was observed at multiple doses of virus (less than 50% mortality per dose), and no dose was associated with either uniform mortality or survival. Brains were taken from four representative mice that had clinical signs of WNV disease, and viral RNA was isolated and sequenced. Upon sequencing of the NS4B region, viral RNA from two of the mice was found to encode an additional NS4B A95T substitution in addition to the original P38G and T116I substitutions. Viral RNA from the brain of a third mouse encoded an additional NS4B V110A mutation while viral RNA isolated from the fourth mouse brain encoded an additional I224V mutation. Upon analysis of the consensus sequencing chromatogram from the original 96-hour 41 °C virus sample, heterogeneity was observed at nucleotides G/A7198 corresponding to residue 95 and T/C7244 corresponding to residue 110, but not at position A7585 corresponding to residue 224, indicating a mixed population of viruses at the 96-hour time point following incubation in Vero cells at 41 °C (data not shown).

To identify any additional mutations within the NS4B region that may have been selected during multiplication at 41 °C, eight plaques were harvested from virus at the 96-hour time point at 41 °C. Nucleotide sequencing of the NS4B region of these eight plaques revealed four isolates encoding the I224V substitution, and one isolate each encoding the following substitutions: A83S, A95T, A100V, and V110A. Thus, A95T, V110A, and I224V substitutions were identified both in plaque picks from the 96-hour time point sample in cell

culture and in mouse brain, while A83S and A100V substitutions were identified only by plaque picking. Virus encoding either a direct G38P or I116T reversion was never detected.

Analysis of compensatory mutants

Viruses containing the engineered P38G/T116I/N480H substitutions in addition to a putative compensatory substitution (i.e., either A83S, A95T, A100V, V110A, or I224V) were analyzed to determine if the temperature-sensitive and/or mouse neuroinvasive-attenuated phenotypes of the parental virus were conserved. Viruses encoding A95T, A100V, V110A, or I224V substitutions in addition to P38G/T116I/N480H were found to be no longer temperature-sensitive in Vero cells at 41 °C with less than a 1 $\log_{10}$ decrease in titer at 41 °C compared to 37 °C, but all multiplied to a lower titer than the wild-type virus at 37 °C (Table 3). The P38G/T116I/N480H + A83S virus was found to be slightly temperature-sensitive with a 1.3 $\log_{10}$ pfu/mL decrease in titer 41 °C versus 37 °C, although this virus was less temperature-sensitive than the parental P38G/T116I/N480H virus and below the 2.0 $\log_{10}$ pfu/mL decreased level denoted as significant. Viruses encoding the putative compensatory substitutions in addition to the P38G/T116I/N480H substitutions were inoculated into three-week-old female NIH Swiss mice via the ip route. Viruses encoding additional A95T, A100V, V110A, and I224V substitutions were found to exhibit mouse-neuroinvasive virulent phenotypes with ip LD_{50} values greater than one million-fold lower than observed for the attenuated P38G/T116I/N480H parental virus (Table 3). The P38G/T116I/N480H/A83S virus was found to retain an attenuated phenotype with an ip LD_{50} value of greater than 1000 pfu. Each P38G/T116I/N480H-derived virus that encoded an additional NS4B compensatory substitution was subjected to complete genomic sequencing, and each virus had the A6049C nucleotide change encoding an NS3 N480H amino acid substitution.

Mutation rate of the NS4B gene of P38G/T116I/N480H virus when passaged in Vero cells at 37 °C or 41 °C

To better understand the significance of the observed compensatory substitutions, viral RNA was isolated from the parental P38G/T116I/N480H virus that had been passaged once in Vero cells post-transfection plus virus samples taken from Vero cell supernatants at 96 h post-infection at 37 °C and 41 °C. Viral RNA was subjected to RT-PCR utilizing NS4B-specific primers, and PCR products were sequenced directly to obtain the consensus sequence. In addition, PCR products were cloned and 21–23 clones were sequenced for each product to assay the prevalence of nucleotide changes and deduced amino acid substitutions. The basal variability of the parental P38G (nucleotide substitutions C7027G and C7028G)/T116I (nucleotide substitution C7262T) viral RNA was analyzed and compared to the selection of specific mutants following 96 h in Vero cells at either 37 °C or 41 °C. Cloned PCR fragments from the parental P38G/T116I/N480H virus were found to exhibit few differences with 3/22 (14%) sequenced fragments exhibiting nucleotide changes and 1/22 (5%) fragment encoding an amino acid substitution (Table 4). Two parental cDNA clones exhibited silent nucleotide changes, and a single cDNA clone encoded a H58Y (C7087T) amino acid substitution. In contrast, 22/23 (96%) cDNA clones from the 96-hour 41 °C virus sample exhibited nucleotide changes leading to amino acid substitutions. Fifteen of 23 (65%) sequenced clones encoded the A95T (G7198A) substitution, 4/23 (17%) encoded the

A100V (C7214T) substitution, 2/23 (9%) encoded the I224V (A7585G) substitution, and 1/23 (4%) encoded a R84Q (G7166A) substitution. In addition, T48A (A7057G), L56P (T7056C), V155I (G7378A), I168V (A7414G), and C227R (T7594C) substitutions were each detected in one cDNA clone (4% prevalence) from the 96-hour 41 °C virus and occurred in conjunction with either an A95T or A100V substitution (Table 4). Seven of 23 (30%) cDNA clones exhibited additional silent nucleotide changes in addition to encoding amino acid substitutions. Sequenced cDNA clones from the 96-hour 37 °C virus sample yielded an intermediate frequency of substitutions with 7/21 (33%) exhibiting nucleotide changes and 5/21 (24%) encoding amino acid substitutions. Two of 21 (10%) clones were found to encode T109A (A7240G) and I245V (A7648G) substitutions. One clone of 21 (5%) encoded a V217I (G7564A) substitution, and another (1/21; 5%) encoded a N189S (A7481G) substitution. Finally, one clone (5%) was found to lack the parental T116I substitution, but this clone encoded an additional M177L (A7444T) substitution. Overall, a total of 50 nucleotide changes were found in 66 cDNA clones that were sequenced, and 49/50 (98%) were transition mutations. The single A7444T transversion led to the deduced M177L amino acid substitution in the only fragment lacking the parental T116I (C7262T) substitution. Three of 50 (6%) nucleotide changes occurred in cDNA clones from the parental virus, 36/50 (72%) occurred in clones from the 96-hour 41 °C virus, and 11/50 (22%) occurred in clones from the 96-hour 37 °C virus.

RNA and protein levels in wild-type and P38G/T116I/N480H virus-infected Vero cells

To investigate the block in viral replication with respect to the multiplication of P38G/T116I/N480H virus at 41 °C, intracellular viral RNA and protein levels were assayed in Vero cells at both 37 °C and 41 °C. Quantitative real-time RT-PCR indicated that levels of viral RNA synthesis for both wild-type and P38G/T116I/N480H viruses were within 100-fold of each other in Vero cells at 37 °C during all time points (Fig. 3A, left panel). In contrast, there was a sharp reduction in synthesis of viral RNA levels in P38G/T116I/N480H virus-infected cells compared to wild-type virus-infected cells (decreases between 1000-fold and 10,000-fold) at 41 °C (Fig. 3A, right panel). Viral protein levels were measured by Western blot utilizing a rabbit anti-WNV E protein domain III antiserum to probe cell lysates generated from virus-infected Vero cells. Viral E protein (~50 kDa band) levels for both wild-type and P38G/T116I/N480H virus-infected cells were similar at 37 °C, while viral protein levels were sharply reduced in P38G/T116I/N480H virus-infected cells compared to wild-type virus-infected cells at 41 °C (Fig. 3B). β-actin (~45 kDa band) was used as an internal standard, and these protein levels were similar in all samples.

Discussion

In this study we have investigated the role of various amino acid substitutions in the NS4B protein and their role in a number of phenotypic properties of WNV. These engineered mutations were focused on a highly conserved N-terminal motif and a central hydrophobic region. Targeted N-terminal residues are highly conserved throughout both tick-borne and mosquito-borne flaviviruses. In contrast, those targeted to the central hydrophobic region are less conserved and exhibit significant variability throughout the *Flavivirus* genus, but have been reported to be involved in phenotypic properties of other flaviviruses. In particular,

there is evidence to suggest that the central region of NS4B plays a role in the virulence phenotype of flaviviruses (Hanley et al., 2003; McArthur et al., 2003; Wicker et al., 2006). Most engineered substitutions were well-tolerated, even those corresponding to positions found to confer altered growth phenotypes in other flaviviruses. Only one of nine recombinant mutant viruses tested exhibited an attenuated phenotype in mice. This mutant, containing an engineered P38G substitution and an additional T116I substitution, was found to exhibit small-plaque morphology, temperature sensitivity at 41 °C, and attenuation of neuroinvasiveness in mice.

The P38G/T116I/N480H mutant exhibited at least 10,000,000-fold attenuation for neuroinvasiveness when inoculated via the ip route, yet was as neurovirulent as wild-type WNV when injected via the ic route. Previously, we reported a recombinant WNV virus containing an NS4B C102S substitution that was highly attenuated for both neuroinvasiveness and neurovirulence (Wicker et al., 2006). The difference in neurovirulence phenotypes between the two attenuated mutants implies that mouse neuroinvasiveness and neurovirulence phenotypes are encoded by different molecular determinants. In addition, while the P38G/T116I/N480H virus exhibited small-plaque morphology, the C102S virus had a large-plaque phenotype. Both viruses were found to be temperature-sensitive at 41 °C although the phenotype was more severe with the C102S virus. The C102 residue resides within the central hydrophobic region that was also targeted in this study suggesting that while most substitutions are well-tolerated, some can significantly alter virulence and multiplication phenotypes.

The engineered P38G substitution is primarily responsible for observed differences in phenotypes as mutants containing NS4B T116I (Table 1A) or NS3 N480H (Table 1B) alone exhibited multiplication and virulence phenotypes similar to those of wild-type WNV, as did the mutants encoding additional NS4B compensatory substitutions (Table 3). The viremia curve showed that the P38G/T116I/N480H virus attained significant serum titers but did not successfully invade the brain (Table 2). It is hypothesized that the attenuated mutant never reached sufficiently high titers to cross the blood–brain barrier. This is further supported by the observation of a highly neurovirulent phenotype following ic inoculation of the P38G/T116I/N480H mutant demonstrating that this virus is fully capable of causing disease following introduction into the central nervous system. Virulent WNV strains have previously been associated with increased viremias and mortality in crows, while attenuated viruses tend to produce lower viremias and concurrent increases in survival (Brault et al., 2007; Kinney et al., 2006). However, it has also been demonstrated that WNV infections successfully crossing the blood–brain barrier do not always result in significant mortality in mice (Brown et al., 2007; Wicker et al., 2006).

Given that virus encoding only the P38G substitution was never isolated following multiple transfection attempts, an additional substitution (such as T116I) may be required for the viability of the virus. To further address this possibility, a P38A substitution was engineered. The resulting recombinant virus did not encode T116I or any additional substitutions, nor did it encode temperature sensitive or mouse attenuated phenotypes. This was expected as the Brazilian flavivirus Ilheus encodes an alanine at the homologous residue suggesting that this substitution would be tolerated (Figueiredo, 2000). It is possible that increased

flexibility introduced by the glycine residue near the putative N-terminal membrane insertion point (see Fig. 2) disrupted the normal conformation provided by proline while the alanine substitution may preserve the natural conformation thereby ablating the need for additional compensatory substitutions. In addition it was found that the attenuated phenotype conferred by the P38G substitution could be compensated by a variety of additional substitutions. Multiplication of the P38G/T116I/N480H virus at 41 °C resulted in identification of variants containing compensatory mutations at the 96-hour time point sample. Viruses containing A95T, A100V, V110A, or I224V substitutions in addition to the original P38G and T116I substitutions exhibited mouse virulence characteristics similar to wild-type WNV and were no longer temperature-sensitive. However, a virus containing an additional A83S substitution was still attenuated for neuroinvasiveness in mice and exhibited a temperature-sensitive phenotype in Vero cells at 41 °C; although this virus was less temperature-sensitive than the parental P38G/T116I/N480H virus. These data suggest that the same underlying mechanism may be responsible for both the temperature-sensitive phenotype in cell culture and the neuroinvasive phenotype in mice. Full-length genomic sequencing was conducted on the P38G/T116I/N480H virus as well as P38G/T116I/N480H derived strains encoding compensatory substitutions, and only the NS3 N480H mutation was observed outside of the NS4B region. While the attenuated phenotype of the P38G/T116I/N480H virus was reversed by a variety of compensatory mutations, a direct G38P revertant was never detected; rather, the engineered substitution appeared to be quite stable. This is presumably due to the engineered glycine differing from proline by two adjacent transversion nucleotide changes (C7027G and C7028G), such that direct reversion would be a rare event. Interestingly, the proline did not mutate to an alanine, which would only require a single nucleotide change, however, this may be due to the presence of the T116I substitution. This is in marked contrast to the previously described C102S (G7220C) virus, where direct S102C (C7220G) revertants (a single nucleotide change) were associated with reversal of temperature-sensitive and mouse attenuation phenotypes (Wicker et al., 2006). Each of the compensatory mutations associated with the engineered P38G virus (A83S (G7162T), A95T (G7198A), A100V (C7214T), V110A (T7244), T116I (C7262T), I224V (A7585G)) represents a single nucleotide change. It is not entirely clear how the compensatory substitutions exert their effects. None of the compensatory mutations were highly conserved among the mosquito-borne flaviviruses. The NS4B A83S substitution has been found to occur naturally in a WNV strain isolated from human plasma in Ohio in 2002 (Davis et al., 2005). In addition, the related naturally mouse-attenuated Rabensburg virus differs from the NY99 strain of WNV at positions A95S, A100V, and T116A (Bakonyi et al., 2005). A lineage 2 isolate from Nigeria also encodes A100V and T116A substitutions while an attenuated lineage 2 strain from Madagascar (MAD78) encodes the T116I substitution, although it is unlikely that this mutation is directly responsible for the attenuation of the virus (Keller et al., 2006; Yamshchikov et al., 2001). In contrast, the V110 and I224 residues are highly conserved in all WNV isolates analyzed to date but not in other members of the JE serogroup.

Putative compensatory substitutions such as T116I, M177L, A95T, A100V, V100A, and I224V may restore the ability of the NS4B protein to assemble and function properly. Yu et al. have shown that there are molecular determinants in both N-terminal and C-terminal

regions of the Hepatitis C virus (HCV) NS4B protein that may influence the ability of NS4B to polymerize (Yu et al., 2006). In addition, it has been shown that substitutions in predicted ER-lumenal regions of the NS4B protein can nearly abolish HCV replicon colony formation although these regions are thought to be separate from the cytoplasmic components of the replication complex (Lindstrom et al., 2006). This is further support for the hypothesis that the NS4B protein may form either oligomers or crucial complexes with certain cellular proteins. While HCV NS4B displays little sequence homology with WNV NS4B, it is thought that these proteins may exhibit similar topologies and functions within the cell (Lundin et al., 2003; Welsch et al., 2007). The P38 residue is predicted to localize to the junction of an ER-lumenal region and a transmembrane domain, and it will be critical to elucidate potential protein–protein interactions to better explain the temperature sensitive and mouse attenuation phenotypes observed in conjunction with disruption of this residue.

The results reported in this study begin to identify the interacting network of residues in WNV NS4B that are essential in maintaining the life cycle of wild type NY99 WNV. In the absence of atomic structural information of NS4B, one cannot provide an accurate interpretation of the current data. However, the data unequivocally establish the presence of long range interactions among various putative structural elements in NS4B. Regardless of the algorithm used in predicting the secondary structures, including the transmembrane domains, there is a consensus that the N-terminal residues reside in the ER lumen and the other key residues involved in this study, e.g. 83, 95, 100, 110, 116 and 224, are located in transmembrane domain(s) (Miller et al., 2007). Thus, residue 38 obviously resides at a distance from the residues that are located in transmembrane domains. It is possible to eliminate a direct pairwise interaction between residue 38 and the others as the likely mechanism to confer compensatory effects as reported in this study. One possible mechanism is the alteration of pairwise interaction between the mutated side-chains and other residues between these putative transmembrane domains. The proof of this mechanism will require the atomic structure of NS4B. Another possibility is that these side-chain substitutions affect the stability of the transmembrane domains (Adamian and Liang, 2001). It has been shown that a single amino acid replacement can affect the stability of a transmembrane domain and as a consequence leading to a disease state (Li et al., 2006). In addition to compensatory mutations observed within the NS4B protein, a NS3 N480H substitution was present in all P38G-derived viruses. Second-site mutations have also been identified within the NS3 protease region of GBV-B RNAs containing NS4B C-terminal HCV amino acid sequences, providing evidence for interaction between NS3 and NS4B during replication (Benureau et al., 2010). The dengue NS4B protein has also been shown to interact with NS3, and it is possible that the engineered WNV NS4B P38G substitution induced the second-site NS3 N480H mutation to preserve the potential for productive interaction during replication (Umareddy et al., 2006). Thus, an understanding of the molecular mechanism of structure–function correlation of NS4B and potential interactions with other host and viral products requires further biophysical studies on the structure and energetics among these elements.

Materials and methods

Site-directed mutagenesis

The 3′ plasmid of the WNV infectious clone WN/IC P991 served as the template for introduction of mutations (Beasley et al., 2005; Kinney et al., 2006). Mutagenesis was conducted using the QuickChange XL Site-Directed Mutagenesis Kit (Stratagene) following the manufacturer's protocol. Sets of primers were designed for each engineered mutation (D35E, P38G, P38A, W42F, Y45F, L97M, A100V, L108P, T116I) including sufficiently long flanking regions to obtain a predicted melting temperature of at least 78 °C. Primer sequences are available upon request. Mutagenesis reactions were carried out in a thermocycler following specific cycling parameters listed in the manufacturer's protocol. Products were then digested with *Dpn*I to remove parental DNA and transformed into XL-10 Gold ultracompetent cells that were plated on Luria-Bertani/ampicillin plates. Four colonies from each mutagenesis reaction were isolated, and plasmid DNA was purified utilizing the GenElute Plasmid Miniprep kit (Sigma). Sequencingwas conducted to confirmthe presence of the desiredmutation and absence of additional mutations in the NS4B gene. Appropriate plasmids were grown in 200 mL cultures to obtain concentrated DNA for further manipulation.

Construction and transfection of recombinant viruses

The WNV NY-99 infectious clone was constructed in two plasmids (Beasley et al., 2005; Kinney et al., 2006). Three micrograms each of 5′ pWN-AB and 3′ pWN-CG infectious clone plasmids were digested simultaneously with *NgoMIV* and *XbaI* restriction enzymes (New England Biolabs). Appropriate DNA fragments were visualized on an agarose gel and purified using a Qiaquick gel extraction kit (Qiagen). Fragments were ligated overnight at room temperature using T4 DNA ligase (NEB). DNA was linearized by digesting with *XbaI*, treated with Proteinase K (Roche), and extracted twice with phenol/chloroform/isoamyl alcohol and once with chloroform. DNA was ethanol precipitated, and the pellet was resuspended in TE buffer. The resulting product served as the template for transcription using a T7 Ampliscribe kit (Epicentre) and A-cap analog (NEB). Following a 3-hour incubation at 37 °C, the transcription reaction was added to 1.5×10^7 African green monkey kidney Vero cells suspended in 500 μL PBS, and transfection was accomplished using electroporation. The cells were placed in a cuvette (0.2 cm electrode gap) on ice, pulsed twice at 1.5 kV, infinite Ohms, and 25 μF, incubated at room temperature for 10 min, transferred to 75-cm^2 flasks containing MEM with 8% FBS, and incubated at 37 °C and 5% CO_2. Viruses were harvested on day 5 or 6 post-transfection, when CPE was evident. Culture medium containing virus was clarified by centrifugation for 5 min at 12,000 g, and 1-mL aliquots were stored at −80 °C. Viral RNA was extracted using the QIAamp Viral RNA Mini-Spin kit (Qiagen). The presence of the engineered NS4B mutation was confirmed by amplifying the NS4B region using the Titan One-Step RT-PCR kit (Roche) and DNA sequencing. Full-length genomic sequencing was conducted of the P38G/T116I/N480H mutant virus to check for additional mutations.

Plaque and temperature sensitivity assays

Infectivity titers of recombinant viruses were determined by plaque titration in Vero cells at both 37 °C and 41 °C. Vero cells were allowed to grow to approximately 90% confluency in six-well plates. Growth medium (MEM with Earle's salts and L-glutamine (Gibco) supplemented with 8% fetal bovine growth serum (FBS) (Hyclone), 100 units/mL penicillin (Gibco), and 100 μg/mL streptomycin (Gibco) was removed, and cells were rinsed with phosphate buffered saline (PBS-Gibco). Serial dilutions of each virus were adsorbed, 200 μL per well, for 30 min before overlaying the cell monolayer with a 50:50 mixture of 2% agar (Sigma) and 2× MEM (Gibco) containing 4% FBS. Two days following the first agar overlay, 2 mL of a mixture of 2% agar and 4% FBS 2× MEM containing 2% neutral red was added to each well. Plaques were visualized and counted the following day, and viral infectivity titers were calculated. Viruses found to be temperature sensitive at 41 °C (i.e., a > 100-fold reduction of efficiency of plaquing compared to that at 37 °C) were plaqued at 39.5 °C to better define the temperature sensitive phenotype.

Mouse virulence studies

Recombinant viruses were diluted in PBS, and 10-fold serial doses ranging from 10^3 pfu to 10^{-1} pfu were injected by ip route in a volume of 100 μL into groups of five 3–4 week old female NIH Swiss mice (Harlan). Clinical signs of infection such as ruffled fur or hunched posture were noted during the following 14 days, and the LD_{50} value was calculated for each virus. Three weeks following inoculation, surviving mice were challenged intraperitoneally with a uniformly lethal dose (100 LD_{50}) of wild-type NY-99 WNV to determine if they had developed a protective immune response. If a virus was found to be attenuated via the ip route, serial 10-fold doses were administered to isofluorane anesthetized 3–4 week old mice in a 20μL volume via the intracerebral (ic) route to investigate the mouse neurovirulence phenotype.

Virus multiplication in cell culture

Growth curves were conducted for wild-type WNV and the mutant viruses in monkey kidney Vero cells at both 37 °C and 41 °C, in mouse neuroblastoma Neuro2A cells at 37 °C, and in mosquito C6/36 cells at 28 °C. Cells were grown in six-well plates in appropriate media and were infected with 200 μL of virus diluted in PBS at a moi of 0.01. After adsorbing virus for 30 min, the cells were washed three times with PBS, and 4 mL of the appropriate medium was added. At various timepoints following infection, 0.5 mL samples were removed and frozen at −80 °C. The harvested samples were then plaque titrated in twelve-well plates of Vero cells. Vero cells were grown in MEM with Earle's salts and L-glutamine (Gibco) supplemented with 8% FBS, 100 units/mL penicillin, and 100 μg/mL streptomycin. Neuro 2A cells were grown in MEM with Earle's salts and L-glutamine supplemented with 8% FBS, 100 units/mL penicillin, 100 μg/mL streptomycin, 0.075% sodium bicarbonate (Sigma), and 1 mM sodium pyruvate (Sigma). C6/36 cells were grown in MEM with Earle's salts and L-glutamine supplemented with 8% FBS (Hyclone), 100 units/mL penicillin, 100 μg/mL streptomycin, and 0.075% tryptose phosphate broth.

Virus multiplication in mice

Female 3–4 week old NIH Swiss mice were inoculated with 100 pfu of either wild-type WNV or P38G/T116I/N480H virus via the ip route. Three mice were sacrificed for each virus per day for 6 days. Blood was collected by cardiac puncture, and brains were harvested. Brains were homogenized by repeated pipetting in 0.5 mL MEM media supplemented with 8% FBS, and centrifuged homogenate supernatants were subjected to plaque assays to determine infectivity titers in the brain. The limit of detection was 2.7 $\log_{10}$ pfu/brain. Viral RNA was also isolated from brains using the Viral RNA Mini Spin kit (Qiagen) and amplified by RT-PCR utilizing the Titan kit (Roche) to detect low levels of virus in the brain below the level of detection for plaque assays. Blood from cardiac puncture was spun down, and serum was removed and frozen. Serum samples were plaque assayed to determine viral titers, and the limit of detection was 1.7 $\log_{10}$ pfu/mL.

Analysis of quasispecies in viral-RNA with respect to compensatory substitutions

Viral RNA was isolated from the parental P38G/T116I/N480H viral stock in addition to virus samples from the 96-hour time point in Vero cells incubated at either 37 °C and 41 °C utilizing the Qiagen RNeasy mini kit. RT-PCR was conducted on the 96-hour time point samples utilizing the Titan RT-PCR kit (Roche) and NS4B-specific primers, and PCR products were cloned into the T-easy vector (Promega). Resulting plasmids were transformed into *E. coli* DH5α cells and selected on LB/ampicillin plates. Twenty-one to 23 colonies each were picked from the parental sample used to infect Vero cell cultures, 96-hour 37 °C sample, and 96-hour 41 °C sample. The NS4B region was sequenced for each cDNA clone, and frequencies of nucleotide and encoded amino acid substitutions for the cDNA clones from each of the three samples were determined.

Quantitative real-time RT-PCR and Western blots

Virus-infected Vero cell monolayers (moi of 0.01) were rinsed three times with PBS, and total viral and cellular RNA was isolated from cellular lysates at 0, 12, 24, and 48 h post-infection by using the Qiagen RNeasy Mini kit. A ~100-bp fragment of the 3′ noncoding region was amplified using TaqMan one-step RT-PCR as described by Vanlandingham et al. (2004) using a primer set first described by Lanciotti et al. (2000). RNA levels were quantified by comparison to a standard curve generated from serial 10-fold dilutions of WNV RNA isolated from a virus stock of known infectivity titer resulting in values expressed as pfu equivalents. To determine protein levels, cell lysates were generated by solubilizing virus- or mock-infected Vero monolayers in 0.5 mL of RIPA buffer containing 1% SDS. Equal volumes (8 μL) of each lysate were run in 12.5% SDS-PAGE gels and transferred to PVDF membranes in duplicate. One membrane was probed with rabbit polyclonal anti-WNV envelope domain III antibody to determine viral E protein levels, while the other membrane was probed with mouse anti-β-actin antibody (Sigma) to assay cellular protein levels.

Acknowledgments

We would like to thank Shinji Makino for helpful discussions related to this work. JAW is supported by NIH T32AI 7526 and this work was supported, in part, by the Clayton Foundation for Research. JCL is supported by the Robert A. Welch Foundation.

References

Adamian L, Liang J. Helix–helix packing and interfacial pairwise interactions of residues in membrane proteins. J. Mol. Biol. 2001; 311:891–907. [PubMed: 11518538]

Ambrose RL, Mackenzie JM. West Nile virus differentially modulates the unfolded protein response to facilitate replication and immune evasion. J. Virol. 2011; 85:2723–2732. [PubMed: 21191014]

Arai M, Mitsuke H, Ikeda M, Xia JX, Kikuchi T, Satake M, Shimizu T. ConPredII: a consensus prediction method for obtaining transmembrane topology models with high reliability. Nucleic Acids Res. 2004; 32:390–393.

Bakonyi T, Hubalek Z, Rudolf I, Nowotny N. Novel flavivirus or new lineage of West Nile virus, central Europe. Emerg. Infect. Dis. 2005; 11:225–231. [PubMed: 15752439]

Beasley DW, Li L, Suderman T, Barrett AD. Mouse neuroinvasive phenotype of West Nile virus strain varies depending upon virus genotype. Virology. 2002; 296:17–23. [PubMed: 12036314]

Beasley DW, Whiteman MC, Zhang S, Huang CY, Schneider BS, Smith DR, Gromowski GD, Higgs S, Kinney RM, Barrett AD. Envelope protein glycosylation status influences mouse neuroinvasion phenotype of genetic lineage 1 West Nile virus strains. J. Virol. 2005; 79:8339–8347. [PubMed: 15956579]

Benureau Y, Warter L, Malcolm BA, Martin A. A comparative analysis of the substrate permissiveness of HCV and GBV-B NS3/4A proteases reveals genetic evidence for an interaction with NS4B protein during genome replication. Virology. 2010; 406:228–240. [PubMed: 20701941]

Blaney JE, Manipon GG, Firestone CY, Johnson DH, Hanson CT, Murphy BR, Whitehead SS. Mutations which enhance the replication of dengue virus type 4 and an antigenic chimeric dengue virus type 2/4 vaccine candidate in Vero cells. Vaccine. 2003; 21:4317–4327. [PubMed: 14505914]

Brault AC, Huang CY, Langevin SA, Kinney RM, Bowen RA, Ramey WN, Panella NA, Holmes EC, Powers AM, Miller BR. A single positively selected West Nile viral mutation confers increased virogenesis in American crows. Nat. Genet. 2007; 39:1162–1166. [PubMed: 17694056]

Brinton MA. The molecular biology of West Nile Virus: a new invader of the western hemisphere. Annu. Rev. Microbiol. 2002; 56:371–402. [PubMed: 12142476]

Brown AN, Kent KA, Bennett CJ, Bernard KA. Tissue tropism and neuroinvasion of West Nile virus do not differ for two mouse strains with different survival rates. Virology. 2007; 368:422–430. [PubMed: 17675128]

Davis CT, Beasley DW, Guzman H, Siirin M, Parsons RE, Tesh RB, Barrett AD. Emergence of attenuated West Nile virus variants in Texas, 2003. Virology. 2004; 330:342–350. [PubMed: 15527859]

Davis CT, Ebel GD, Lanciotti RS, Brault AC, Guzman H, Siirin M, Lambert A, Parsons RE, Beasley DW, Novak RJ, Elizondo-Quiroga D, Green EN, Young DS, Stark LM, Drebot MA, Artsob H, Tesh RB, Kramer LD, Barrett AD. Phylogenetic analysis of North American West Nile virus isolates 2001–2004: evidence for the emergence of a dominant phenotype. Virology. 2005; 342:252–265. [PubMed: 16137736]

Evans JD, Seeger C. Differential effects of mutations in NS4B on West Nile virus replication and inhibition of interferon signaling. J. Virol. 2007; 81:11809–11816. [PubMed: 17715229]

Figueiredo LT. The Brazilian flaviviruses. Microbiol. Infect. 2000; 2:1643–1649.

Hahn CS, Dalrymple JM, Strauss JH, Rice CM. Comparison of the virulent Asibi strain of yellow fever virus with the 17D vaccine strain derived from it. Proc. Natl. Acad. Sci. U. S. A. 1987; 84:2019–2023. [PubMed: 3470774]

Hanley KA, Manlucu LR, Gilmore LE, Blaney JE Jr. Hanson CT, Murphy BR, Whitehead SS. A trade-off in replication in mosquito versus mammalian systems conferred by a point mutation in the NS4B protein of dengue virus type 4. Virology. 2003; 312:222–232. [PubMed: 12890635]

Keller BC, Fredericksen BL, Samuel MA, Mock RE, Mason PW, Diamond MS, Gale M Jr. Resistance to alpha/beta interferon is a determinant of West Nile virus replication fitness and virulence. J. Virol. 2006; 80:9424–9434. [PubMed: 16973548]

Khromykh AA, Sedlak PL, Westaway EG. trans-Complementation analysis of the flavivirus Kunjin ns5 gene reveals an essential role for translation of its N-terminal half in RNA replication. J. Virol. 1999; 73:9247–9255. [PubMed: 10516033]

Kinney RM, Huang C-Y, Whiteman MC, Bowen RA, Langevin SA, Miller BR, Brault AC. Avian virulence and thermostable replication of the North American strain of West Nile virus. J. Gen. Virol. 2006; 87:3611–3622. [PubMed: 17098976]

Kuno G, Chang GJ. Biological transmission of arboviruses: reexamination of and new insights into components, mechanisms, and unique traits as well as their evolutionary trends. Clin. Microbiol. Rev. 2005; 18:608–637. [PubMed: 16223950]

Lanciotti RS, Kerst AJ, Nasci RS, Godsey MS, Mitchell CJ, Savage HM, Komar N, Panella NA, Allen BC, Volpe KE, Davis BS, Roehrig JT. Rapid detection of West Nile virus from human clinical specimens, field-collected mosquitoes, and avian samples by a TaqMan RT-PCR assay. J. Clin. Microbiol. 2000; 38:4066–4071. [PubMed: 11060069]

Li E, You M, Hristova K. FGFR3 dimer stabilization due to a single amino acid pathogenic mutation. J. Mol. Biol. 2006; 356:600–612. [PubMed: 16384584]

Lindstrom H, Lundin M, Haggstrom S, Persson MA. Mutations of the Hepatitis C virus protein NS4B on either side of the ER membrane affect the efficiency of subgenomic replicons. Virus Res. 2006; 121:169–178. [PubMed: 16806556]

Lundin M, Monne M, Widell A, von Heijne G, Persson MA. Topology of the membrane-associated Hepatitis C virus protein NS4B. J. Virol. 2003; 77:5428–5438. [PubMed: 12692244]

Mastrangelo E, Milani M, Bollati M, Selisko B, Peyrane F, Pandini V, Sorrentino G, Canard B, Konarev PV, Svergun DI, de Lamballerie X, Coutard B, Khromykh AA, Bolognesi M. Crystal structure and activity of Kunjin virus NS3 helicase; protease and helicase domain assembly in the full length NS3 protein. J. Mol. Biol. 2007; 372:444–455. [PubMed: 17658551]

McArthur MA, Suderman MT, Mutebi JP, Xiao SY, Barrett AD. Molecular characterization of a hamster viscerotropic strain of Yellow Fever virus. J. Virol. 2003; 77:1462–1468. [PubMed: 12502861]

Miller S, Sparacio S, Bartenschlager R. Subcellular localization and membrane topology of the dengue virus type 2 non-structural protein 4B. J. Biol. Chem. 2006; 281:8854–8863. [PubMed: 16436383]

Miller S, Kastner S, Krijase-Locker J, Buhler S, Bartenschlager R. The non-structural protein 4A of dengue virus is an integral membrane protein inducing membrane alterations in a 2K-regulated manner. J. Biol. Chem. 2007; 282:8873–8882. [PubMed: 17276984]

Mukhopadhyay S, Kuhn RJ, Rossmann MG. A structural perspective of the flavivirus life cycle. Nat. Rev. Microbiol. 2005; 3:13–22. [PubMed: 15608696]

Munoz-Jordan JL, Sanchez-Burgos GG, Laurent-Rolle M, Garcia-Sastre A. Inhibition of interferon signaling by dengue virus. Proc. Natl. Acad. Sci. U. S. A. 2003; 100:14333–14338. [PubMed: 14612562]

Munoz-Jordan JL, Laurent-Rolle M, Ashour J, Martinez-Sobrido L, Ashok M, Lipkin WI, Garcia-Sastre A. Inhibition of Alpha/Beta interferon signaling by the NS4B protein of flaviviruses. J. Virol. 2005; 79:8004–8013. [PubMed: 15956546]

Ni H, Chang GJ, Xie H, Trent DW, Barrett AD. Molecular basis of attenuation of neurovirulence of wild-type Japanese encephalitis virus strain SA14. J. Gen. Virol. 1995; 76:409–413. [PubMed: 7844560]

Pletnev AG, Putnak R, Speicher J, Wagar EJ, Vaughn DW. West Nile virus/dengue type 4 virus chimeras that are reduced in neurovirulence and peripheral virulence without loss of immunogenicity or protective efficacy. Proc. Natl. Acad. Sci. U. S. A. 2002; 99:3036–3041. [PubMed: 11880643]

Preugschat F, Strauss JH. Processing of nonstructural proteins NS4A and NS4B of dengue 2 virus in vitro and in vivo. Virology. 1991; 185:689–697. [PubMed: 1683727]

Puig-Basagoiti G, Tilgner M, Bennett CJ, Zhou Y, Munoz-Jordan JL, Garcia-Sastre A, Bernard KA, Shi PY. A mouse cell-adapted NS4B mutation attenuates West Nile virus RNA synthesis. Virology. 2007; 361:229–241. [PubMed: 17178141]

Roosendaal J, Westaway EG, Khromykh A, Mackenzie JM. Regulated cleavages at the West Nile virus NS4A-2K–NS4B junctions play a major role in rearranging cytoplasmic membranes and Golgi trafficking of the NS4A protein. J. Virol. 2006; 80:4623–4632. [PubMed: 16611922]

Umareddy I, Chao A, Sampath A, Gu F, Vasudevan SG. Dengue virus NS4B interacts with NS3 and dissociates it from single-stranded RNA. J. Gen. Virol. 2006; 87:2605–2614. [PubMed: 16894199]

Vanlandingham DL, Schneider BS, Klingler K, Fair J, Beasley D, Huang J, Hamilton P, Higgs S. Real-time reverse transcriptase-polymerase chain reaction quantification of West Nile virus transmitted by Culex pipiens quinquefasciatus. Am.J.Trop. Med. Hyg. 2004; 71:120–123. [PubMed: 15238700]

Wang E, Ryman KD, Jennings AD, Wood DJ, Taffs F, Minor PD, Sanders PG, Barrett AD. Comparison of the genomes of the wild-type French viscerotropic strain of yellow fever virus with its vaccine derivative French neurotropic vaccine. J. Gen. Virol. 1995; 76:2749–2755. [PubMed: 7595382]

Welsch C, Albrecht M, Maydt J, Herrmann E, Welker MW, Sarrazin C, Scheidig A, Lengauer T, Zeuzem S. Structural and functional comparison of the non-structural protein 4B in flaviviridae. J. Mol. Graph. Model. 2007; 26:546–557. [PubMed: 17507273]

Westaway EG, Khromykh AA, Kenney MT, Mackenzie JM, Jones MK. Proteins C and NS4B of the flavivirus Kunjin translocate independently into the nucleus. Virology. 1997; 234:31–41. [PubMed: 9234944]

Wicker JA, Whiteman MC, Beasley DW, Davis CT, Zhang S, Schneider BS, Higgs S, Kinney RM, Barrett AD. A single amino acid substitution in the central portion of the West Nile virus NS4B protein confers a highly attenuated phenotype in mice. Virology. 2006; 349:245–253. [PubMed: 16624366]

Yamshchikov VF, Wengler G, Perelygin AA, Brinton MA, Compans RW. An infectious clone of the West Nile flavivirus. Virology. 2001; 281:294–304. [PubMed: 11277701]

Yu G, Lee K, Gao L, Lai MM. Palmitoylation and polymerization of Hepatitis C virus NS4B protein. J. Virol. 2006; 80:6013–6023. [PubMed: 16731940]

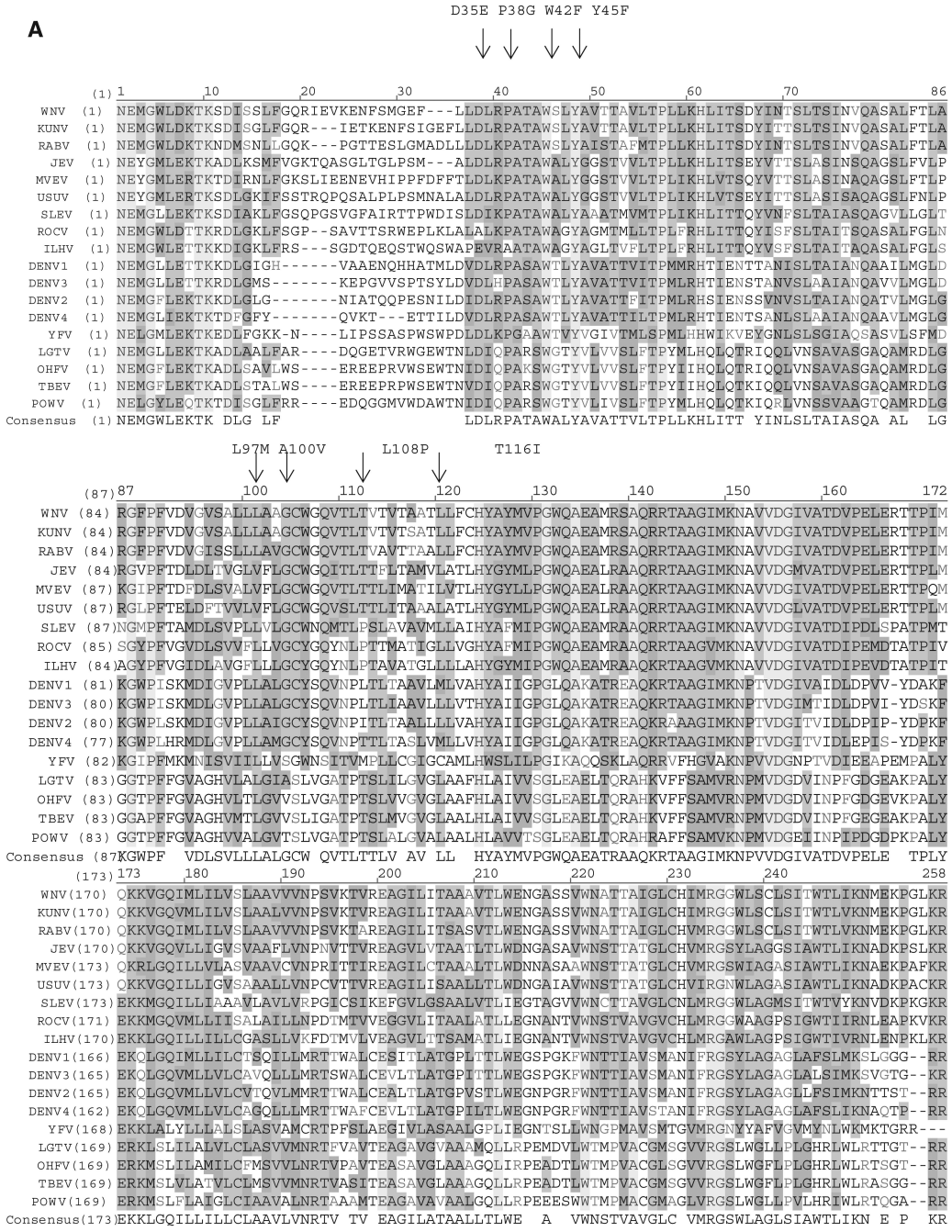

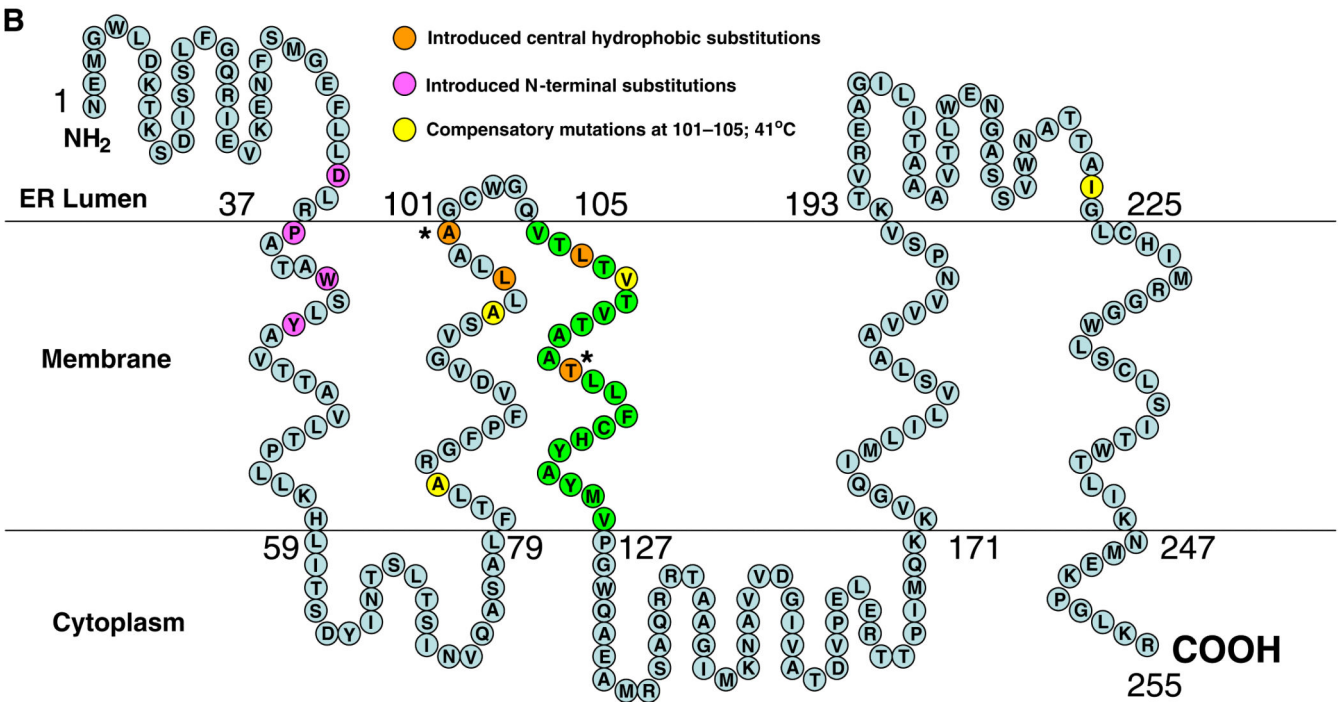

Fig. 1.

Primary amino acid sequence of NS4B proteins from different flaviviruses and predicted secondary structure of WNV NS4B. (A) Complete NS4B amino acid alignments including both tick-borne and mosquito-borne flaviviruses show locations of introduced substitutions in the conserved N-terminal region (D35E, P38G, W42F, Y45F) and central hydrophobic domain (L97M, A100V, L108P, T116I). Virus abbreviations: WNV: West Nile NY99 strain (NC_009942); KUNV: Kunjin (AY274504); RABV: Rabensburg (AY765264); JEV: Japanese encephalitis (NC_001437); MVEV: Murray Valley encephalitis (NC_000943); USUV: Usutu (NC_006551); SLE: St. Louis encephalitis (NC_007580); ILHV: Ilheus (NC_009028); ROCV: Rocio (AY632542); DEN1: dengue 1 (NC_001477); DEN2: dengue 2 (NC_001474); DEN3: dengue 3 (NC_001475); DEN4: dengue 4 (NC_002640); YFV: yellow fever Asibi strain (AY640589); LGTV: Langat (NC_003690); OHFV: Omsk hemorrhagic fever (NC_005062); TBEV: Tick-borne encephalitis (NC_001672); POWV: Powassan (L06436). (B) A topological model was constructed based on the consensus prediction (ConPredII) hydrophobicity plotting program (Arai et al., 2004). Five transmembrane domains were predicted, and amino acids 106–126 represent the primary transmembrane domain (green). Predicted locations of introduced N-terminal substitutions are shown in purple while introduced central hydrophobic substitutions are shown in orange. Positions of additional compensatory substitutions (A83S, A95T, A100V, V110A, I224V) observed in the P38G/T116I/N480H virus incubated at 41 °C are shown in yellow. *A100V and T116I substitutions were introduced as central hydrophobic substitutions but also represent compensatory substitutions following introduction of the P38G substitution.

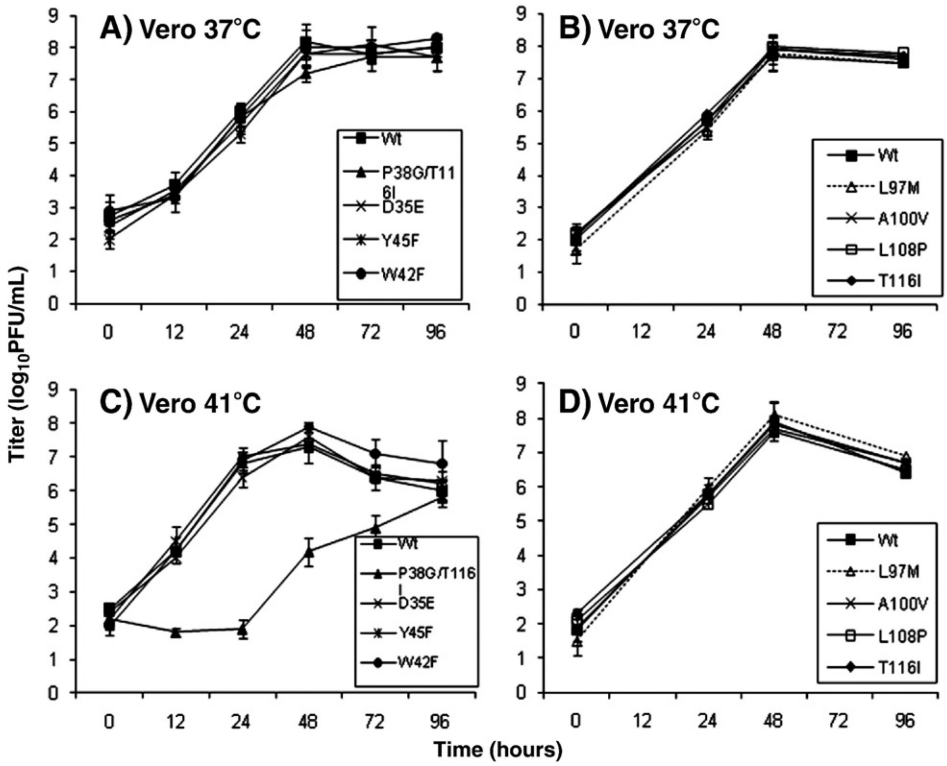

Fig. 2.

Multiplication kinetics of recombinant wild-type and N-terminal or central hydrophobic mutant viruses in monkey kidney Vero cells. Growth curves were conducted at a MOI of 0.01, and the limit of detection was ≤0.7 $\log_{10}$ pfu/mL. N-terminal (A) and central hydrophobic (B) mutants in Vero cells at 37 °C, N-terminal (C) and central hydrophobic (D) mutants in Vero cells at 41 °C.

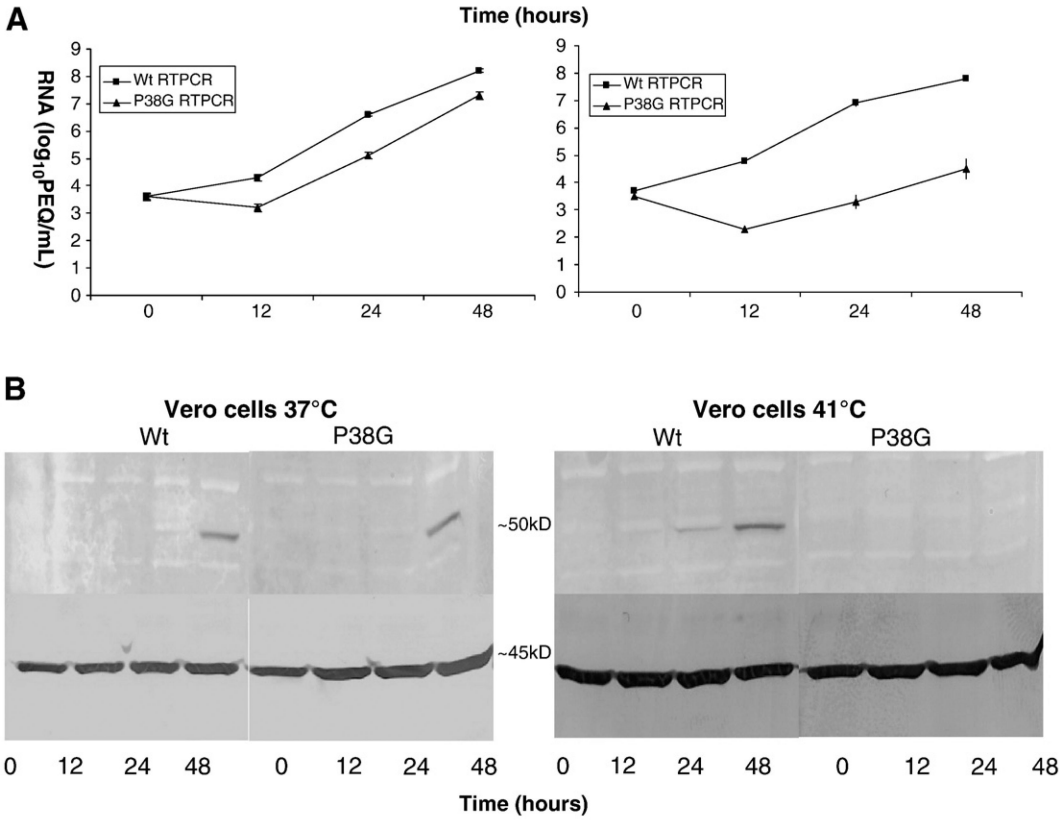

Fig. 3.

Viral RNA (A) and protein (B) levels from cell lysates of wild-type and P38G/T116I/N480H mutant infected cell cultures incubated at 37 °C and 41 °C. (A) TaqMan quantitative real-time RT-PCR was conducted on total cellular RNA preparations using primers localizing to the WNV 3′-UTR. Data were converted to pfu equivalents (PEQ) utilizing a standardized curve. (B) Protein levels were assayed from crude cellular lysates, and Western blots were probed for WNV E protein (~50 kDa band) with rabbit anti-E domain III polyclonal antibody. β-actin (~45 kDa band) levels were used as an internal standard.

Table 1

Mouse virulence and temperature sensitive phenotypes of recombinant wild-type WNV, the central hydrophobic mutants, and the N-terminal mutants (A) and the recombinant wild-type WNV, attenuated P38G/T1161/N480H and N480H (B).

Virus[c]	Mouse virulence[a]			Temperature sensitivity[b]		
	i.p. LD_{50} (pfu)	i.p. AST (days±SD)	i.c. LD_{50} (pfu)	Viral titer/mL at 37 °C (log_{10} pfu)	Viral titer/mL at 41 °C (log_{10} pfu)	Relative change in viral titer [log_{10} (pfu 41 °C/pfu 37 °C)]
A						
NY99	0.5	7.4±0.9	<0.1	6.5	6.7	−0.2
D35E	0.4	7.2±0.9	n.d.	5.7	5.4	−0.3
P38G/T116I/N480H	>10,000	>35	<0.1	6.2	2.4	−3.8
W42F	<0.1	7.4±0.9	n.d.	6.7	6.5	−0.2
Y45F	<0.1	7.4±0.9	<0.1	5.5	5.8	0.3
L97M	0.4	7.6±1.0	n.d.	6.5	6.8	0.3
A100V	0.7	7.2±0.4	n.d.	7.0	6.7	−0.3
L108P	<0.1	7.6±1.5	n.d.	6.8	7.0	0.2
T116I	0.7	8.0±1.8	n.d.	6.9	7.0	0.1
P38A	7	8.6±1.5	n.d.	5.8	5.6	−0.2
B						
NY99	80	8.3±0.5	n.d.	7.2	7	0.2
N480H	20	8.2±0.5	n.d.	6.5	6	0.5
P38G/T1161/N480H	>100,000	>18	n.d.	n.d	n.d	n.d.

n.d.=not done.

[a] Median lethal viral dose (LD50) or median protective viral dose (PD_{50}) following intraperitoneal (i.p.) or intracerebral (i.c.) administration of virus. AST=average survival time.

[b] Virus seeds were plaque titrated in Vero cells under agar overlay at 37 °C and 41 °C. The relative change [log_{10} (titer at 41 °C/titer at 37 °C)] in viral titer at the higher temperature indicates the degree of temperature sensitivity.

[c] Infectious clone-derived wild-type WNV, strain NY99, central hydrophobic mutants, and N-terminal mutants in NS4B were tested. D35E=aspartic acid-to-glutamic acid mutation at amino acid residue NS4B-38.

Table 2

Viremia and brain titers from mice inoculated with 100 pfu of either wild-type WNV or P38G/T116I/N480H mutant virus via the intraperitoneal route.

Day	NY99 ip serum (log_{10} pfu/mL)	Brain titer (log_{10} pfu/brain)	P38G/T116I ip serum (log_{10} pfu/mL)	Brain titer (log_{10} pfu/brain)
1	4.1±0.9	_ [a]	2.5±0.3	–
2	5.0±0.5	–	3.1±0.2	–
3	2.5±0.3	–	2.3±0.6	–
4	2.1±0.1	4.3±0.3	2.0 [b]	–
5	–	5.1±0.8	–	–
6	–	6.8±0.6	–	–

[a] No virus detected. The limits of detection were 1.7 log_{10}pfu/mL in the serum and 2.7 log_{10}pfu/brain.

[b] Only one of three mice had detectable infectivity.

Table 3

Temperature sensitive and mouse virulence phenotypes of P38G/T116I/N480H-derived viruses encoding compensatory substitutions.

Virus[c]	Temperature sensitivity[a]			Mouse virulence[b]	
	Viral titer/mL at 37 °C (log_{10}pfu)	Viral titer/mL at 41 °C (log_{10} pfu)	Relative change in viral titer [$log_{10}(pfu_{41C}/pfu_{37C}$]	i.p. LD_{50} (pfu)	i.p. AST (days±SD)
NY99	7.2	7.0	−0.2	0.7	7.2±0.4
P38G/T116I/N480H	6.7	3.4	−3.3	>10,000,000	>35
+A83S	4.7	3.4	−1.3	>1000	>21
+A95T	5.0	4.6	−0.4	2.0	8.8±0.8
+A100V	5.5	5.1	−0.4	8.0	11±1.2
+V110A	5.1	4.7	−0.4	4.0	9.6±1.3
+I224V	4.6	4.3	−0.3	5.0	11±2.0

[a] Virus seeds were plaque titrated in Vero cells under agar overlay at 37 °C and 41 °C. The relative change [log_{10} (titer at 41 °C/titer at 37 °C)] in viral titer at the higher temperature indicates the degree of temperature sensitivity.

[b] Median lethal viral dose (LD50) following intraperitoneal (i.p.) administration of virus. AST=average survival time.

[c] Infectious clone-derived wild-type NY99 WNV, attenuated P38G/T116I/N480H virus, and P38G/T116I/N480H-derived viruses encoding additional amino acid substitutions. +A83S=alanine-to-serine mutation at amino acid residue NS4B-83 in addition to NS4B P38G, T116I , and NS3 N480H substitutions.

Table 4

Analysis of the mutation rate of the NS4B gene of P38G/T116I/N480H virus during replication in Vero cells at either 37 °C or 41 °C compared to sequence variability in the parental stock.

cDNA clone no.[b]	Parental P38G/T116I virus[a]		37 °C 96-hour virus		41 °C 96-hour virus	
	Nucleotide change	Amino acid change	Nucleotide change	Amino acid change	Nucleotide change	Amino acid change
1	–	_ [c]	–	–	A7158G, G7198A*[d], G7378A*	A95T, V155I
2	–	–	–	–	T7015C, C7214T*	A100V
3	T7015C	–	G7564A*	V217I	G7198A*	A95T
4	–	–	G7080A	–	G7198A*, T7488C, A7554G	A95T
5	C7087T*	H58Y	–	–	G7198A*	A95T
6	–	–	–	–	G7198A*	A95T
7	–	–	G7080A, A7240G*, A7648G*	T109A, I245V	G7198A*	A95T
8	–	–	–	–	G7198A*	A95T
9	–	–	–	–	G7198A*	A95T
10	–	–	A7218G	–	G7198A*	A95T
11	–	–	–	–	C7214T*, A7227G	A100V
12	–	–	–	–	T7015C, C7214T*, T7594C*	A100V, C227R
13	–	–	–	–	G7166A*	R84Q
14	–	–	A7481G*	N189S	G7198A*	A95T
15	–	–	–	–	G7198A*, C7410T, A7417G*	A95T, I168V
16	–	–	–	–	A7005G, G7198A*, T7488C	A95T
17	–	–	–	–	A7585G*	I224V
18	–	–	A7240G*, A7648G*	T109A, I245V	G7198A*	A95T
19	–	–	–	–	G7198A*	A95T
20	–	–	T7262C*, A7444T*	I116T, M177L	A7057G*, C7214T*	T48A, A100V
21	A7554G	–	–	–	–	–
22	–	–	N.A.	N.A.	A7585G*	I224V
23	N.A.	N.A.	N.A.	N.A.	T7056C*, G7198A*	L56P, A95T

*=nucleotide mutation(s) that encode the shown amino acid mutation(s).

[a] Parental virus passaged once in Vero cells following the initial derivation by transfection.

[b] RT-PCR-amplified cDNA containing the NS4B gene was cloned into a plasmid vector in *E. coli*. The nucleotide sequences of 21 or 23 individual NS4B clones were analyzed for the presence of non-engineered mutations.

[c] –=no nucleotide mutation detected in the cloned NS4B gene fragment.

[d] =nucleotide mutation(s) that encode the shown amino acid mutation(s).